

The direct influence of retinal degeneration on electrical stimulation efficacy: Significant implications for retinal prostheses

Author:

Ly, K; Lovell, NH; Muralidharan, M; Italiano, ML; Tsai, D; Shivdasani, MN; Guo, T; Dokos, S

Publication details:

Proceedings of the Annual International Conference of the IEEE Engineering in Medicine and Biology Society, EMBS

v. 00

Medium: Print

pp. 1 - 4

9798350324471 (ISBN)

1557-170X (ISSN); 2694-0604 (ISSN)

Event details:

2023 45th Annual International Conference of the IEEE Engineering in Medicine & Biology Society (EMBC)

United States

2023-07-24 - 2023-07-27

Publication Date:

2023-01-01

Publisher DOI:

<https://doi.org/10.1109/EMBC40787.2023.10340724>

License:

<https://creativecommons.org/licenses/by/4.0/>

Link to license to see what you are allowed to do with this resource.

Downloaded from http://hdl.handle.net/1959.4/unsworks_85141 in <https://unsworks.unsw.edu.au> on 2024-04-28

The direct influence of retinal degeneration on electrical stimulation efficacy: Significant implications for retinal prostheses

Keith Ly, *Student Member, IEEE*, Nigel H. Lovell, *Fellow, IEEE*, Madhuvanathi Muralidharan, Michael L. Italiano, David Tsai, *Senior Member, IEEE*, Mohit N. Shivdasani, *Senior Member, IEEE*, Tianruo Guo, *Senior Member, IEEE*, Socrates Dokos, *Member, IEEE*

Abstract— Photoreceptor loss and inner retinal network remodeling severely impacts the ability of retinal prosthetic devices to create artificial vision. We developed a computational model of a degenerating retina based on rodent data and tested its response to retinal electrical stimulation. This model includes detailed network connectivity and diverse neural intrinsic properties, capable of exploring how the degenerated retina influences the performance of electrical stimulation during the degeneration process. Our model suggests the possibility of quantitatively modulating retinal ON and OFF pathways between phase II and III of retinal degeneration without requiring any differences between ON and OFF RGC intrinsic cellular properties. The model also provided insights about how remodeling events influence stage-dependent differential electrical responses of ON and OFF pathways.

Clinical Relevance—This data-driven model can guide future development of retinal prostheses and stimulation strategies that may benefit patients at different stages of retinal disease progression, particularly in the early and mid-stages, thus increasing their global acceptance.

I. INTRODUCTION

Despite significant recent engineering advances in retinal prosthetic devices that aim to replace the function of photoreceptors lost in inherited retinal dystrophies by artificially activating retinal neurons, functional outcomes in recipients have been largely underwhelming [1, 2]. As a result, existing devices are prescribed only to patients with profound vision impairment. Until the prosthetic vision quality is significantly improved, most patients who could benefit from the uptake of such technology, simply remain ‘waiting’ for an alternative appropriate treatment.

Retinal neurons undergo remodeling in disease, leading to altered synaptic connections and neurotransmitter release, as well as functional changes which can strongly influence the ability of electrical stimulation [3-5] in evoking distinct and punctate phosphenes. However, it remains unclear to what degree the stage of retinal degeneration (RD) affects the efficacy of retinal stimulation. Previous studies use post-natal day as the indicator of RD stages without considering the biological variation of the degeneration process across different stages. Several retinal stimulation studies have reported conflicting changes in thresholds of retinal ganglion cells (RGCs) in the degenerate retina, when compared to thresholds recorded in a healthy retina [5, 6]. More recent data

have shown that retinal responses are unpredictable across different stages of disease progression [3, 4]. To better understand the performance of electrical stimulation during the degeneration process, we developed a discrete neuronal network model of retinal electrical stimulation. We hypothesized that the stage of RD could differentially impact the response of ON and OFF RGCs to electrical stimulation given the unique network connections in the two pathways. This model allows us to assess how biophysical and synaptic parameters affect electrically evoked retinal responses over a wide range of degenerative stages.

II. METHODS

A. Discrete Network Model of Retinal Degeneration

A biophysically detailed retinal network including rods, cones, horizontal cells (HZs), rod, ON and OFF bipolar cells (BCs), AII amacrine cells (ACs), and ON and OFF RGCs was implemented in NEURON 7.2. This model includes detailed network connectivity and diverse neural intrinsic properties, capable of accurately simulating remodeling events during progressive photoreceptor and inner retinal degeneration. The model’s performance has been well validated by a wide range of biological recordings across different animal models of RD [7, 8]. More details of model structure, equations and parameters can be found in Ly et al. [9].

To simulate the loss of photoreceptor (PR) outer segments (and subsequent inactivation of mGluR neurotransmitters in ON BCs) in early-stage RD (Phase I/II, Fig. 2A1), we gradually reduced the steady-state depolarizing membrane potential of PRs in the dark condition [10]. Secondary atrophy of the PRs was modeled by gradually reducing the synaptic conductance (mimicking the loss of iGluR neurotransmitters in OFF BCs). In addition, Rod BC-OFF BC “switching”, an important remodeling process identified in Phase II [11], was simulated by removing the synapse between rods and rod BCs. Late-stage RD (Phase III, Fig. 2A2) was modeled by gradually reducing the synaptic conductance between BCs and RGCs as well as the gap junction conductance between ON BCs and AII ACs, mimicking the inner RD process.

B. Epiretinal Electrical Stimulation

A mono-polar circular electrode disk with ground located at infinity was placed in the center of the modelled retinal

K. Ly, N. H. Lovell, M. Muralidharan, M. L. Italiano, D. Tsai, M. N. Shivdasani, T. Guo, and S. Dokos are with the Graduate School of Biomedical Engineering and Tyree Institute of Health Engineering, UNSW Sydney, NSW 2052, Australia.

E-mail for correspondence: keith.ly@unsw.edu.au

tissue 25 μm above the RGC layer (to account for the thickness of the nerve fiber layer [12]). The extracellular domain was homogeneous, hence the extracellular voltage (V) at each spatial point is defined by:

$$V(r, z) = \frac{I_o \rho_e}{2R\pi} \sin^{-1} \left(\frac{2R}{\sqrt{(r-R)^2 + z^2} + \sqrt{(r+R)^2 + z^2}} \right)$$

where r and z are the radial and axial displacement from the centre of the disk for $z \neq 0$ [13]. R is the diameter of the disk (75 μm [5]), I_o is the stimulation current, ρ_e is the extracellular resistivity (500 $\Omega\cdot\text{cm}$) [14]. Electrical stimuli consisted of biphasic charge-balanced cathodic-first current pulses (1 ms per phase) [5]. The stimulus frequency ranged from 10 to 50 pulses per second. The total number of spikes elicited as a function of stimulus amplitude was fit to a sigmoid curve and the RGC activation threshold was defined as the lowest current amplitude required to elicit a 0.5 spiking probability. Threshold values were normalized to RGC thresholds in the wild-type (WT) condition.

C. Whole Cell Patch-Clamping in *rd1* Retina

All procedures were reviewed and approved by the UNSW Animal Care and Ethics committee. Whole-cell patch recordings were conducted in degenerating mouse (*rd1*) retina (post-natal day: P60~P250) based on previous *ex vivo* studies [7, 8]. In brief, excised retinæ were perfused with Ames' medium (Sigma-Aldrich) at 3-4 mL/min, equilibrated with 5% CO_2 / 95% O_2 to pH 7.4 and heated to 33-35 $^\circ\text{C}$. Glass pipettes (Warner Instruments, Hamden, CT, USA) with tip resistances of 3 – 6 $\text{M}\Omega$ were used for patching the RGCs. RGCs were classified as ON or OFF based on two properties: (1) the dendritic stratification within the inner-plexiform layer (IPL), and (2) the distinct patterned activity exhibited by the ON and OFF RGCs.

III. RESULTS

A. Effects of Disease Progression on ON and OFF RGC Electrical Stimulation

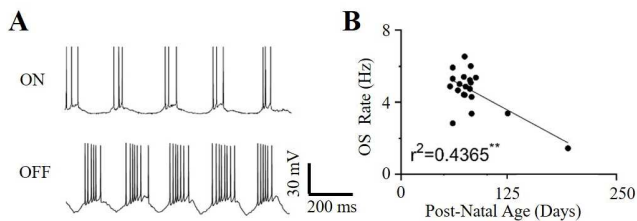


Figure 1. (A) An example of patterned oscillatory activity recorded from ON and OFF RGCs in *rd1* retina at P70. (B) Recorded oscillation frequency over post-natal age of ON ($n = 9$) and OFF ($n = 10$) RGCs.

Our model first simulated the stage-dependent oscillation patterns, which were supported by our *ex vivo* patch-clamping data in *rd1* retina (Fig. 1A and B). It produced a 6.5-Hz oscillation frequency at 100% PR loss (Fig. 2B2), corresponding to P60 in our *rd1* recordings (Fig. 1B). The simulated oscillations were gradually weakened by reducing synapses and gap junctions in the inner retina (Fig. 2B2), corresponding to the 2-Hz oscillation seen at P200 in animals and eventually disappearing at P250 (Fig. 1B).

To demonstrate the effects of degeneration progression on RGC electrical stimulation, we plotted the ON and OFF RGC

thresholds and their oscillatory rates as a function of RD stages (Fig. 2B1-B2). RGC oscillatory activities were categorized as high-rate (> 5 Hz indicated by light orange shadow in Fig. 2B) and low-rate (< 5 Hz indicated by grey shadow in Fig. 2B) [5].

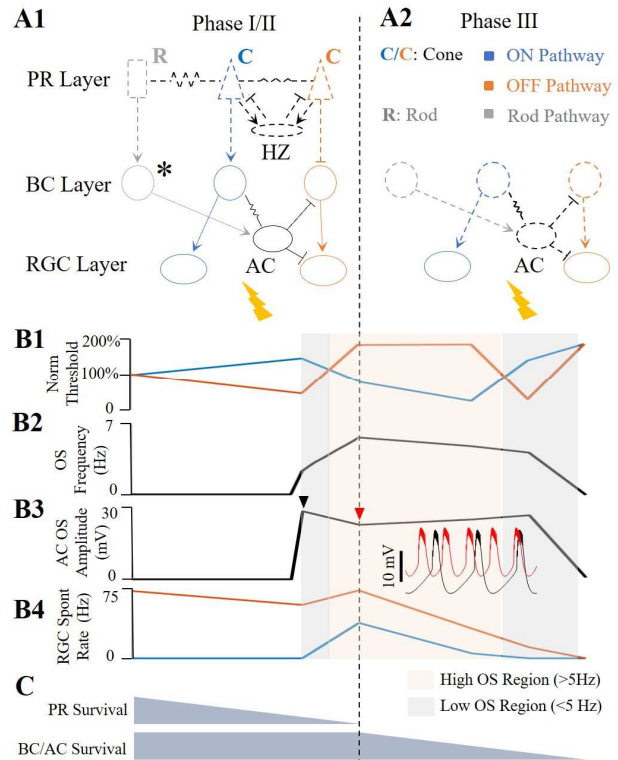


Figure 2. The effects of oscillatory activity at different stages of RD on the electrical stimulation threshold of ON and OFF RGCs (\rightarrow excitatory synapse, $-$ inhibitory synapse, resistor: gap junction). (A1-A2) Discrete network model of PR degeneration (Phase I/II) and inner retinal degeneration (Phase III). Dashed lines indicate a progressive cell death and reduction in synaptic and gap-junction conductance. * The removal of the rod-rod BC synapse simulates the inhibitory effect of rod BC switching. (B1) The impact of photoreceptor loss and inner retinal network changes on epiretinal stimulation thresholds for RGC excitation. ON and OFF RGCs showed a different threshold dependency on RD stage. (B2) Rhythmic oscillatory (OS) activity in RGCs increases as PRs die in Phase I/II of RD and reduces at later stages of RD. (B3) The depolarization amplitude of AC as RD progresses. At low oscillation frequencies (< 5 Hz, grey shadow), the amplitude of the oscillation is larger than at higher oscillation frequencies (> 5 Hz, light orange shadow). insert: AC membrane potential measure at 6.5 Hz (red) and 3 Hz (black). (B4) The rate of spontaneous spiking activity at different stages of RD for both ON and OFF RGCs. (C) To represent the different phases of RD, we assumed a uniform rate of photoreceptor death in Phase I/II as well as constant disconnection of inner retinal synapses in Phase III.

When the modeled RGCs exhibited high-rate oscillations (Fig. 2 light orange region) in response to RD, the ON RGC exhibited a similar or lower threshold to electrical stimulation than WT conditions. This is consistent with existing studies, where high-rate oscillatory activity did not increase the threshold of RGCs [5, 15]. Interestingly, our model's OFF RGC exhibited an inverse stage-dependent activity, suggesting an overall elevated threshold compared to WT conditions. In contrast, under low-rate oscillations induced by RD (Fig. 2B2, grey shadow), the model's ON RGC exhibited a higher threshold than WT, during both early and late-stage RD. This result has been previously identified in *rd10* retina

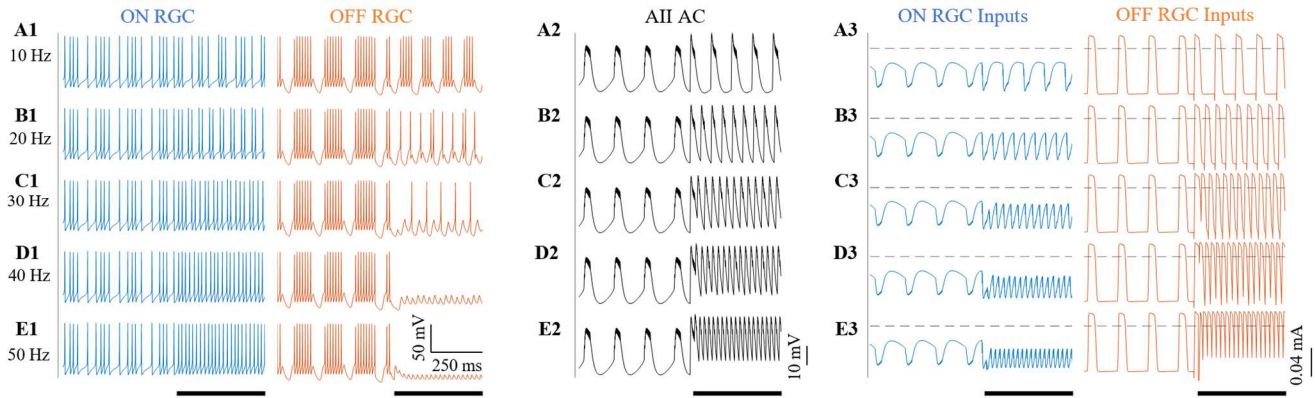


Figure 3. Differential stimulation of ON and OFF RGCs using 10-50 Hz epiretinal stimulation after 100% loss of PRs. (A1-E1) ON and OFF RGCs exhibited spontaneous monophasic and biphasic rhythmic activity after 100% loss of PRs before the onset of stimulus. Electrical stimulus depolarized the ON RGC whilst hyperpolarizing the OFF RGC, causing an inverse effect between the two cells. This effect was maximized by increasing the stimulus frequency. (A2-E2) Higher frequency stimulation caused a more depolarized membrane potential in the AC. (A3-E3) ON and OFF synaptic currents demonstrated characteristic monophasic and biphasic current waveforms (dashed line indicates 0 mA). Higher stimulus frequency (40 and 50 Hz) caused more overall inward synaptic inputs into the ON RGC but more outward inputs to the OFF RGC, resulting in differential ON and OFF stimulation. The stimulus is active during the time highlighted by the black bar under each panel.

[5] but the mechanism(s) for this threshold increase is unclear. Again, the model's OFF RGC had inverse stage-dependent activity compared to the ON RGC, showing a lower threshold in both early and later stages of RD.

To examine possible mechanisms underlying the RD stage-dependent RGC thresholds, we simulated the AC oscillation frequency (Fig. 2B2) and peak-to-peak amplitude (Fig. 2B3) at different stages of RD. Under low-rate oscillatory activity in RGCs, the AC peak-to-peak oscillation amplitude was ~ 7 mV larger than found when RGCs exhibited high-rate oscillatory activity (Fig. 2B3, insert: AC membrane potential at 6.5 Hz and 3 Hz oscillation). These differential AC oscillation amplitudes could cause different fluctuation levels in RGC baseline potentials, further influencing their thresholds. In Fig. 2B4, fluctuations in RGC baseline potential cause an increase/decrease in the spontaneous spiking rate in RGCs.

B. Effects of Stimulus Frequency on RGC response

The differential ON and OFF threshold values in Fig. 2B1 suggest the possibility of selective ON and OFF activation at specific RD stages. To investigate whether RGC oscillatory activity could be modulated by electrical stimulation, we applied $1.5 \mu\text{A}$ electrical stimulation (suprathreshold for the ON RGC but subthreshold for the OFF RGC) at varying frequencies between 10 and 50 Hz, in increments of 10 Hz (Fig. 3), to the RD condition with the highest oscillatory activity (100% PR loss, where inner retinal network was intact). Fig. 3A1-E1 shows the membrane potential of the ON and OFF RGCs before and after onset of stimulation (indicated by the black bar). Electrical stimulation dominated the RGC activity by forcing RGC spikes to follow the electrical stimulus as opposed to firing in an oscillatory behavior. More importantly, electrical stimulation increased the ON RGC spiking activity while inhibiting spontaneous oscillatory activity in the OFF RGC. Increasing stimulus frequency up to 40 or 50 Hz entirely blocked activity in the OFF RGC, maximizing the differential activation between the two pathways (Fig3. D1 and E1).

Fig. 3A2-E2 shows the increasingly depolarized AC, induced by the higher stimulus frequency. This resulted in increased excitatory input to the ON pathway and increased inhibitory input to the OFF pathway. Fig. 3A3-E3 demonstrates the modelled synaptic current input to ON and OFF RGCs, indicating an increasingly stronger net inward current into the ON RGC and a more outward current into the OFF RGC, thus possibly explaining the mechanisms behind the observed differential activation.

IV. DISCUSSION AND CONCLUSION

Existing retinal prosthetic devices are currently prescribed only for patients at very late stages of RD ($\sim 0.46\%$ of all retinitis pigmentosa patients [16]). This study not only provides insights into why devices implanted in late-stage patients are not as effective as originally thought, but also provides a motivation for considering implanting at an earlier stage during the disease. After validating the model with a range of biological data recorded in degenerated retina, this study suggests the possibility of differentially modulating ON and OFF pathways before inner retinal remodeling occurs. Thus, our results shed light on how our stimulation method may benefit patients at the early and mid-degenerative stages when treatment may be most needed.

A. ON and OFF Pathways Displayed Characteristic Stage-Dependent Stimulus-Response Relationships

A recent study recorded different RGC responses in rd10 retina [5]. Their data suggested that low-rate (< 5 Hz) cells had a higher threshold compared to WT, while high-rate (~ 6 Hz) cells had a comparable or lower threshold relative to their WT counterparts [5]. As well as closely replicating these experimental observations, our model provides insights that differences in thresholds may be caused by different AC membrane fluctuations between high- and low-rate oscillations. More importantly, our model predicts the stage-dependent differential ON and OFF electrical response which has not been conveyed clearly in prior retinal stimulation

studies, suggesting that this effect is dominated by differential network mediated input changes during remodeling events.

Since our model's ON and OFF RGCs share identical intrinsic properties, the difference in threshold was purely due to network mediated synaptic inputs into RGCs. During early-stage RD when RGCs exhibit low oscillatory activity (Fig 2B1, phase II), Rod BC switching causes loss of excitatory input into the AC, subsequently causing less excitatory input into the ON RGC and less inhibitory input into the OFF RGC. This results in an increased ON RGC threshold and a decreased OFF RGC threshold compared to WT conditions. During later-stage RD when RGCs exhibit low-rate oscillatory activity (Fig 2B1, end of phase III), the increased ON RGC threshold is likely due to the loss of excitatory input from ON BCs (caused by synaptic retraction and BC death) during inner retinal remodeling. Similarly, the OFF RGC loses excitatory input from OFF BCs, resulting in a hyperpolarized membrane potential and reduced spontaneous activity (Fig. 2B4). This reduction in spontaneous activity allows the OFF RGC to be easily stimulated as the overdepolarization induced by high-rate spontaneous activity inhibits electrically elicited spikes.

In addition, the high-oscillation rate ON RGC (at 100% PR loss stage) initially exhibited a similar threshold to its WT counterpart, with a reduced threshold as inner RD progressed (Fig. 2B1, light orange region). The reduced ON RGC threshold correlates with the reduction in spontaneous spike rate at more advanced stages of RD (Fig. 2B4) in the ON RGC. In contrast, the high-rate oscillating OFF RGC exhibited an initially elevated threshold due to the AC depolarization (Fig. 2B3), resulting in an increase of inhibitory input to both the OFF BC and RGC. As inner RD progresses, although AC inhibitory input is reduced, BC excitatory input is also reduced (Fig. 2B4, OFF RGC spontaneous spiking is reduced), thereby maintaining the elevated OFF RGC threshold.

B. Differentially Modulating ON and OFF Pathways between Phase II and III

Our model predicts the possibility of differentially modulating retinal ON and OFF pathways between Phase II and III of RD. By utilizing higher frequency stimulation (up to 40 and 50 Hz), the OFF RGC was silent whilst the ON RGC was activated (Fig. 3D1, E1). In our simulation, epiretinal stimulation depolarized the AC (Fig. 3D2, E2), subsequently causing stronger excitatory inputs into the ON RGC (through the ON BC) and stronger inhibitory inputs into the OFF RGC from the network (Fig. 3 D3, E3), resulting in a more depolarized ON RGC and a hyperpolarized OFF RGC. These results suggest that epiretinal stimulation may be advantageous to patients with a largely surviving inner retinal network. Inner retinal synaptic retraction occurring in later stages would diminish this network-driven selectivity.

Finally, our results could be beneficial for understanding how RD affects electrical stimulation in the human retina. Much like rodents, human/primate retina exhibit different response profiles through a variety of factors, such as neural types and network connections. These factors are the basis of

differential ON and OFF activation during electrical stimulation [7, 8, 17-19] and are applicable across different species.

In summary, this study enables a more informed retinal stimulation design by improving the ability to predict the effects of combining electrical stimulation with remodeled retinal pathways at different RD stages, allowing more clinically relevant stimulation strategies to be developed.

V. REFERENCES

- [1] L. N. Ayton, N. Barnes, G. Dagnelie, T. Fujikado, G. Goetz *et al.*, "An update on retinal prostheses," *Clin Neurophysiol*, vol. 131, no. 6, pp. 1383-1398, 2020
- [2] T. Guo, M. N. Shivdasani, D. Tsai, L. N. Ayton, D. L. Rathbun *et al.*, "Visual Prostheses: Neuroengineering Handbook," in *Handbook of Neuroengineering*, N. V. Thakor, Ed. Singapore:Springer, 2021
- [3] Y. J. Yoon, J. I. Lee, Y. J. Jang, S. An, J. H. Kim *et al.*, "Retinal degeneration reduces consistency of network-mediated responses arising in ganglion cells to electric stimulation," *IEEE Trans Neural Syst Rehabil Eng*, vol. 28, no. 9, pp. 1921-1930, 2020
- [4] C. Seongkwang, A. Jungryul, J. Yurim, L. Yong Hee, K. Hyong Kyu *et al.*, "Stage-dependent changes of visual function and electrical response of the retina in the rd10 mouse model," *Front. Cell. Neurosci.*, 2022
- [5] A. Cho, C. Ratliff, A. Sampath, and J. Weiland, "Changes in ganglion cell physiology during retinal degeneration influence excitability by prosthetic electrodes," *J Neural Eng*, vol. 13, no. 2, p 025001, 2016
- [6] C. Sekirnjak, C. Hulse, L. H. Jepson, P. Hottoway, A. Sher *et al.*, "Loss of responses to visual but not electrical stimulation in ganglion cells of rats with severe photoreceptor degeneration," *J Neurophysiol*, vol. 102, no. 6, pp. 3260-9, 2009
- [7] D. J. Margolis, G. Newkirk, T. Euler, and P. B. Detwiler, "Functional stability of retinal ganglion cells after degeneration-induced changes in synaptic input," *J Neurosci*, vol. 28, no. 25, pp. 6526-36, 2008
- [8] D. J. Margolis, A. J. Gartland, J. H. Singer, and P. B. Detwiler, "Network oscillations drive correlated spiking of ON and OFF ganglion cells in the rd1 mouse model of retinal degeneration," *PLoS One*, vol. 9, no. 1, p e86253, 2014
- [9] K. Ly, T. Guo, D. Tsai, M. Muralidharan, M. N. Shivdasani *et al.*, "Simulating the impact of photoreceptor loss and inner retinal network changes on electrical activity of the retina," *J Neural Eng*, vol. 19, 2022
- [10] D. Attwell, F. S. Werblin, and M. Wilson, "The properties of single cones isolated from the tiger salamander retina," *J Physiol*, vol. 328, pp. 259-83, 1982
- [11] R. Marc, B. W. Jones, J. Anderson, K. Kinard, D. W. Marshak *et al.*, "Neural reprogramming in retinal degenerations," *Invest Ophthalmol Vis Sci.*, vol. 48, no. 7, p 8, 2007
- [12] L. R. Ferguson, J. M. Dominguez, S. Balaiya, S. Grover, and K. V. Chalam, "Retinal thickness normative data in wild-type mice using customized miniature SD-OCT," *PLoS One*, vol. 8, p e67265, 2013
- [13] S. Dokos and T. Guo, "Computational Models of Neural Retina," in *Encyclopedia of Computational Neuroscience*, D. Jaeger and R. Jung, Eds. New York:Springer, 2020
- [14] J. K. Mueller and W. M. Grill, "Model-based analysis of multiple electrode array stimulation for epiretinal visual prostheses," *J Neural Eng*, vol. 10, no. 3, p 036002, 2013
- [15] R. J. Jensen and J. F. Rizzo, 3rd, "Activation of ganglion cells in wild-type and rd1 mouse retinas with monophasic and biphasic current pulses," *J Neural Eng*, vol. 6, no. 3, p 035004, 2009
- [16] C. M. Vezinaw, G. A. Fishman, and J. J. McAnany, "Visual impairment in retinitis pigmentosa," *Retina*, vol. 40, no. 8, pp. 1630-1633, 2020
- [17] M. Muralidharan, T. Guo, M. N. Shivdasani, D. Tsai, S. Fried *et al.*, "Neural activity of functionally different retinal ganglion cells can be robustly modulated by high-rate electrical pulse trains," *J Neural Eng*, vol. 17, no. 4, 2020
- [18] T. Guo, D. Tsai, J. W. Morley, G. J. Suaning, T. Kameneva *et al.*, "Electrical activity of ON and OFF retinal ganglion cells: a modelling study," *J Neural Eng*, vol. 13, no. 2, p 025005, 2016
- [19] C. Y. Yang, D. Tsai, T. Guo, S. Dokos, G. J. Suaning *et al.*, "Differential electrical responses in retinal ganglion cell subtypes: effects of synaptic blockade and stimulating electrode location," *J Neural Eng*, vol. 15, no. 4, p 046020, 2018